Fluorine-19 NMR Spectroscopic Studies of Phenyl-fluorinated Iron Tetraarylporphyrin Complexes

Byungho Song* and Byung-soo Yu†

Department of Chemistry, Sunmoon University, Asan City, ChungNam 336-840, Korea
†Department of Chemistry, Wonkwang University, Iksan, ChunBuk 570-749, Korea
Received March 8, 2003

Fluorine-19 NMR solution measurements have been made for various phenyl-fluorinated iron porphyrin complexes. Large chemical shifts for phenyl fluorine signals of iron(III) and iron(II) are observed, and these signals are sensitive to electronic structure. The chemical shift differences in ortho-phenyl fluorine signals between high-spin ferric and low-spin ferric tetrakis(pentafluorophenyl)porphyrins are approximately 40 ppm, whereas the differences are approximately 7 ppm between high- and low-spin states of ferrous tetrakis(pentafluorophenyl)porphyrin complexes. Analysis of fluorine-19 isotropic shifts for the iron(III) tetrakis(pentafluorophenyl) porphyrin using fluorine-19 NMR indicates there is a sizable contact contribution at the ortho-phenyl fluorine ring position. Large phenyl fluorine-19 NMR chemical shift values, which are sensitive to the oxidation and spin states, can be utilized for identification of the solution electronic structures of iron(III) and iron(II) porphyrin complexes.

Key Words : F-19 NMR, Porphyrin, Contact shift, Isotropic shift, Dipolar shift

Introduction

The NMR spectra of paramagnetic iron porphyrin species are particularly high in information content, and such spectra may be utilized for electronic and molecular structural analysis. Solution structural identification is especially important with regard to the observation of axial ligand signals. Proton and deuterium resonance values with considerations of linewidths provide a diagnostic means for identification of iron porphyrin oxidation, spin and ligation states.[1-3] Well-resolved carbon-13 NMR spectra of the paramagnetic iron porphyrins are also utilized for structural assignments and detailed isotropic-shift analysis.[2,4]

The proton and deuterium NMR chemical shift value for the pyrrole resonance of paramagnetic metallotetraarylporphyrins has proven to be of considerable utility in definition of the electronic structures. However, phenyl proton NMR resonances of the iron tetraarylporphyrins provide less information for elucidation of the iron porphyrin chemistry due to the relatively small dispersion of signals. Improved dispersion of fluorine-19 signals in phenyl-fluorinated iron porphyrin complexes is demonstrated in this report for various spin and oxidation states of iron tetrakis(pentafluorophenyl), tetrakis(2,6-difluorophenyl) and tetrakis(4-fluorophenyl) porphyrin complexes. The iron tetrakis(pentafluorophenyl)porphyrin has unique properties in that the electron-deficient porphyrin induces a high affinity of iron for axial ligands, efficiently stabilizes high-valent iron porphyrin complexes,[5] and therefore serve as an efficient catalyst for oxidation of hydrocarbons.[6-8] Empirical and theoretical correlation of F-19 NMR chemical shifts and iron porphyrin electronic structures will facilitate the continuing utilization of fluorinated iron porphyrin compounds.

Experimental Section

Materials. Chlorinated solvents were purified by previously reported methods.[9] Toluene and dimethylsulfoxide (DMSO) were purchased as distilled-in-glass solvents and further purified by modifications of published methods.[10] Solvents were degassed after or during purification either by purging with nitrogen or by the freeze-pump-thaw method. Deuterated solvents (toluene-d_8, DMSO-d_6, CD_2Cl_2) were purchased from Aldrich and deoxygenated by the freeze-pump-thaw method. Solvents were stored in the argon atmosphere of a dry box.

Methyl-, ethyl- and propylmagnesium bromide and butyl- and phenyllithium were purchased from Aldrich as tetrahydrofuran (THF) or diethyl ether solutions and used without purification. Solid tetrabutylammonium fluoride, $(Bu_4N)F\cdot 3H_2O$, and tetrabutylammonium hydroxide, $(Bu_4N)OH$, as a 1.0 M solution in methanol were purchased from Aldrich.

Iron Porphyrin Synthesis. Tetrakis(pentafluorophenyl)-porphyrin, (F_{20}-$TPPH_2$), and chloroiron(III) tetrakis(pentafluorophenyl)porphyrin, (F_{20}-TPP)Fe(III)Cl, were purchased from Aldrich. Chloroiron(III) tetrakis(2,6-difluorophenyl)-porphyrin ((F_8-TPP)Fe(III)Cl), tetrakis(3,5-difluorophenyl)-porphyrin and tetrakis(4-fluorophenyl)porphyrin (F_4-TPP)-Fe(III)Cl) were prepared by literature methods.[11] Alkyl- and aryliron(III) porphyrins were prepared by stoichiometric addition of alkyllithium, aryllithium or alkylmagnesium bromide to the toluene solutions of the chloroiron(III) porphyrin complexes.[12]

The perchloratoiron(III) tetrakis(2,6-difluorophenyl)porphyrin complexes were produced by equilibration of the hydroxoiron(III) porphyrin complex with aqueous 1.0 M perchloric acid solution.[13] The fluoroiron(III) porphyrin complexes were obtained from the reaction of corresponding μ-oxo dimeric iron(III) porphyrin complexes with 1.0 M

hydrofluoric acid. The difluoroiron(III) tetrakis(2,6-difluorophenyl)porphyrin complex was generated by addition of excess hydrated tetrabutylammonium fluoride salt ($Bu_4NF\cdot 3H_2O$) to (F_8-TPP)Fe(III)F in dichloromethane solution at ambient temperature.[5] Hydroxoiron(III) tetrakis(pentafluorophenyl)porphyrin complexe, (F_{20}-TPP)Fe(III)OH, was generated from (F_{20}-TPP)Fe(II) in toluene solution. Addition of O_2 to (F_{20}-TPP)Fe(II) initially produces hydroxoiron(III) porphyrin, (F_{20}-TPP)Fe(III)OH, and these compounds slowly converts to the dinuclear μ-oxoiron(III) porphyrin in 72 hours in toluene solution. The μ-oxoiron(III) porphyrin precipitated from toluene solution due to the low solubility in this solvent. Precipitated solid product was separated by filtration through a medium glass frit. Re-dissolution of the solid product in CD_2Cl_2 and examination by proton NMR spectroscopy revealed that the 14.0 ppm pyrrole proton signal was characteristic of (F_{20}-TPP)Fe(III)-O-Fe(III)(F_{20}-TPP).[14] Fluoro- and hydroxoiron(II) porphyrin anionic complexes were prepared by addition of the respective tetrabutylammonium salt to the square-planar iron(II) porphyrin.[15,16] Crystalline iron(II) tetrakis(pentafluorophenyl)porphyrins, (F_{20}-TPP)Fe(II) and (F_{20}-TPP)Fe(II)$(THF)_2$, were prepared in the dry box by mercury-activated zinc powder reduction of the chloroiron(III) complex in toluene and tetrahydrofuran solutions, respectively.[17] Iron(II) tetrakis(pentafluorophenyl)porphyrins bis-coordinated by CN^- and piperidine and mono-ligated by Cl^-, $CH_3CO_2^-$ and 2-methylimidazole were prepared by addition of excess NaCN and piperidine and Bu_4NCl, $Bu_4N(CH_3CO_2)$ and 2-methylimidazole to the square-planar iron(II) porphyrin. Employed solvents are listed in Tables. (F_{20}-TPP)Fe(II)CO was prepared from the reaction of 1 atm CO gas with square-planar (F_{20}-TPP)Fe(II) in CD_2Cl_2.

Measurements. Fluorine-19 and proton NMR spectra of iron porphyrin solutions were recorded at 25 °C on Bruker MSL-300 or Bruker AC-300 spectrometers. A fluorine frequency of 282.3 MHz was used. Chemical shifts are referenced to $CFCl_3$ (F-19 NMR) and $(CH_3)_4Si$ (proton NMR) and downfield shifts are given a positive sign. Concentrations of iron porphyrins ranged from 1.0 mM to 10.0 mM.

Results and Discussion

Assignment of Signals. Phenyl proton NMR chemical shift values of representative iron tetraarylporphyrin derivatives are listed in Table 1. Phenyl proton NMR signals of iron porphyrin complexes are often located in the diamagnetic region with small differences in chemical shift values among *ortho*, *meta* and *para* phenyl proton resonances. The exception to this generalization is seen for iron porphyrin radical complexes where large upfield and downfield alternating chemical shifts of phenyl protons are observed.[3,13] Comparatively small chemical shifts of phenyl proton signals and moderately large linewidths limit the general utility of phenyl proton NMR data for identification of electronic structures of iron porphyrins. However, fluorine-19 NMR data for the fluorinated iron porphyrins as shown in Table 2I demonstrate the potential of F-19 NMR spectroscopy as a diagnostic method for identification of iron porphyrin oxidation, spin, and ligation states.

Table 1. Phenyl Proton NMR Data for Various Iron Porphyrin Complexes

Spin & Oxidn states	Species	Pyrrole-H	Phenyl, ppm			Ref
			ortho	meta	para	
H.S. Fe(III)	(TPP)FeCl	79.8[a]	7.0	13.2 12.1	6.3	19
H.S. Fe(III)	(F_8-TPP)FeCl	80.5[b]		10.6 11.5	7.6	11
H.S. Fe(III)	(TPP)FeF_2^-	85.3[b]	10.3	7.8	8.6	13
L.S. Fe(III)	(TPP)FeBu	-18.4[c]	2.45	4.26	5.32	25
H.S. Fe(II)	(TPP)FeF^-	30.3[b]	7.2	7.89 8.02	6.98	14
S=1, Fe(II)	(TPP)Fe	4.6[c]	20.8	12.5	12.5	2
L.S. Fe(II)	(TPP)FeCO	8.9[d]	7.5	8.2	7.5	26

Signals are referenced to $(CH_3)_4Si$. Abbreviations: H. S., high-spin: L. S., low-spin., Bu, C_4H_9. a in $CDCl_3$ solution. b in CD_2Cl_2 solution. c in C_6D_6 solution. d in tol-d_8 solution.

Fluorine-19 NMR spectra for a number of known iron(III) and iron(II) are examined here. The spectrum for (F_{20}-TPP)Fe(III)Cl is shown in Figure 1. Signals were assigned by examination of the 2,6-F and 3,5-F phenyl-substituted analogues and by consideration of linewidths. Broad o-phenyl fluorine signals are located at -102.0 ppm and -105.1 ppm. The meta-phenyl fluorine signals are also split into two

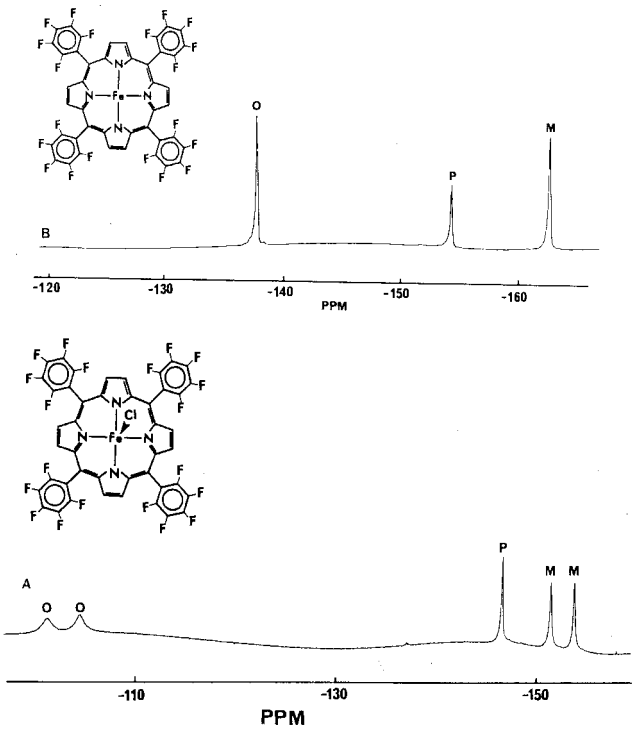

Figure 1. Fluorine-19 NMR spectrum (282.3 MHz) of (A) 5 mM (F_{20}-TPP)Fe(III)Cl in CD_2Cl_2 solution and (B) 5 mM (F_{20}-TPP)Fe(II)$(CN)_2^-$ in DMSO-d_6 solution at 25 °C, chemical shifts referenced to $CFCl_3$.

meta-phenyl fluorine signal splitting is well beyond usual fluorine-fluorine coupling constants, and is best explained by inequivalence of phenyl fluorine groups with respect to axial ligation at the iron center. Phenyl groups are orthogonal to the porphyrin plane and phenyl group rotation is slow on the 282 MHz NMR time scale. Observation of ortho- and/or meta-phenyl fluorine signal splitting provides useful information with regard to the symmetry of axial ligation. However, absence of phenylfluorine signal splitting can not be taken as an indicative of symmetric axial ligation, as the splitting may not be resolved due to large linewidths. Hence, among the five-coordinate high-spin iron(III) derivatives the fluoride and hydroxide complexes show larger linewidths (due to lower zero-field-splitting) than does the chloride complex. Phenyl signal splitting is resolved for the chloride complexes, but none is evident (at 282 MHz) for the fluoride complex and only the meta-fluorine signal is split for (F_8-TPP)Fe(III)OH.

Sizable and often distinctive paramagnetic chemical shifts are evident for phenyl fluorine resonances of high-spin iron(III) porphyrins. For example, downfield shifts of 35.0 and 5.0 ppm are seen for m, p signals, respectively for (F_{20}-TPP)Fe(III)Cl as compared with the metal-free porphyrin or diamagnetic (F_{20}-TPP)Fe(II)CO complex. The ortho-fluoro signal of (F_8-TPP)Fe(III)X is sensitive to the nature of the X ligand as is seen in a 9 ppm difference for the chloride complex as compared with fluoride and hydroxide complexes. The difluoro anionic complex, (F_8-TPP)Fe(III)F_2^-, gives a phenyl-fluoro chemical shift value only slightly upfield from that of the free ligand. The perchlorate complex, (F_8-TPP)-Fe(III)ClO_4, is shown to exhibit an S = 5/2, S = 3/2 spin admixture.[13,18] Thus, it is surprising that the fluoro-phenyl chemical shift value for the perchlorate complex approximates that for the fluoride and hydroxide complexes. No general correlation with ligand properties is yet apparent for the fluoro-phenyl chemical shift values of high-spin iron(III) complexes. The greatly attenuated F-19 paramagnetic shifts seen for the dimeric iron(III) complexes in Table 2 are well understood in terms of the antiferromagnetic coupling through the oxo-bridge.

A group of organometallic complexes of (F_{20}-TPP)Fe(III) were prepared as representative of the low-spin iron(III) state (Table 2). These species are five-coordinate and lack of axial symmetry is associated with splitting of the ortho-phenyl signal (no splitting of the meta-phenyl signal was resolved). Maximum paramagnetic chemical shifts of approximately 9 ppm are seen for the low-spin complexes, and it should be emphasized that shifts are in the upfield direction. Chemical shift differences are quite small among the aryl- and alkyl-(F_{20}-TPP)Fe(III) complexes listed in Table 2. Low-spin bis-imidazole complexes of iron(III) porphyrins have been described extensively,[3] but efforts to generate such complexes of (F_{20}-TPP)Fe(III) resulted in autoreduction to the iron(II) porphyrin.

Fluorine-19 NMR spectra of representative high-spin and low-spin iron(II) tetrakis(pentafluorophenyl)porphyrin complexes are shown in Figure 2. The F-19 NMR spectrum of the S = 2 (F_{20}-TPP)Fe(II)F^- complex in CD_2Cl_2 solution at 25 °C shows split ortho-phenyl fluorine signals at -128.2 ppm and -132.0 ppm. Meta- and para-phenyl fluorine signals are located at -160.9 ppm, -162.5 ppm (meta), and -154.1 ppm (para).

The other two five-coordinate anionic high spin iron(II) complexes exhibit comparable ortho-fluoro chemical shift values, but considerable differences in meta-fluoro signal

Table 2. Fluorine-19 NMR Data of Phenyl-fluorinated Iron Porphyrin Complexes

spin & oxidn states	species	phenyl fluorine, ppm			pyrrole-H
		ortho	meta	para	ppm
Free ligand	(F_{20}-TPPH_2)	-137.3	-162.1	-152.2	[b]
Free ligand	(F_8-TPPH_2)	-109.4			[b]
H. S. Fe(III)	(F_{20}-TPP)FeCl	-102.0	-152.1	-147.2	81.9[b]
		-105.1	-154.6		
H. S. Fe(III)	(F_8-TPP)FeCl	-78.5			80.5[b]
		-81.0			
H. S. Fe(III)	(F_4-TPP)FeCl			-108.0	80.0[b]
H. S. Fe(III)	(F_8-TPP)FeF	-88.3			80.1[b]
H. S. Fe(III)	(F_8-TPP)FeF_2^-	-109.8			85.2[b]
H. S. Fe(III)	(F_4-TPP)FeF			-110.5	80.1[b]
H. S. Fe(III)	(F_{20}-TPP)FeOH	-104.0	-155.0	-148.5	81.0[c]
			-157.0		
H. S. Fe(III)	(F_8-TPP)FeOH	-88.3			80.7[b]
Fe(III) dimer	[(F_{20}-TPP)Fe]$_2$O	-133.9	-162.1	-152.9	14.0[b]
		-136.2	-164.2		
Fe(III) dimer	[(F_8-TPP)Fe]$_2$O	-102.8			13.6[b]
S=5/2 Fe(III) 3/2	(F_8-TPP)FeClO_4	-89.0			35.7[b]
L. S. Fe(III)	(F_{20}-TPP)FePh	-143.8	-164.4	-154.0	-18.5[c]
		-146.2			
L. S. Fe(III)	(F_{20}-TPP)FeBu	-145.4	-164.7	-154.7	-20.2[c]
		-146.5			
L. S. Fe(III)	(F_{20}-TPP)FePr	-143.9	-164.6	-154.5	-21.2[c]
		-145.2			
L. S. Fe(III)	(F_{20}-TPP)FeMe	-143.8	-164.6	-154.4	-20.5[c]
		-146.3			
L. S. Fe(III)	(F_4-TPP)FeEt			-116.5	-18.2[c]
H. S. Fe(II)	(F_{20}-TPP)Fe(THF)$_2$	-140.4	-165.3	-157.7	59.0[e]
H. S. Fe(II)	(F_{20}-TPP)FeF^-	-128.2	-160.9	-154.1	30.1[c]
		-130.2	-162.5		
H. S. Fe(II)	(F_{20}-TPP)$FeOH^-$	-130.2	-156.7	152.4	33.6[c]
			-		
H. S. Fe(II)	(F_{20}-TPP)$FeCl^-$	-131.0	-165.1	-157.9	40.7[c]
		-132.2	-166.0		
H. S. Fe(II)	(F_{20}-TPP)Fe(2-MeIm)	-127.9	-157.9	-149.9	54.3[c]
S=1 Fe(II)	(F_{20}-TPP)Fe	-135.5	-161.4	-152.2	5.8[c]
S=1 Fe(II)	(F_8-TPP)Fe	-105.6			5.0[b]
L. S. Fe(II)	(F_{20}-TPP)Fe(pip)$_2$	-137.9	-163.3	-153.7	8.4[b]
L. S. Fe(II)	(F_{20}-TPP)FeCO	-137.7	-162.3	-152.5	8.9[b]
L. S. Fe(II)	(F_{20}-TPP)Fe$(CN)_2^{2-}$	-137.6	-163.6	-153.2	8.9[b]

a spectra taken at 25 °C, referenced to $CFCl_3$. b in CD_2Cl_2 solution. c in tol-d_8 solution. d in DMSO-d_6 solution. e in THF-d_8 solution. Abbreviation: H. S., high-spin: L. S., low-spin: Ph, C_6H_5: Bu, C_4H_9: Pr, C_3H_7:Et, C_2H_5: Me, CH_3: pip, piperidine: 2-MeIm, 2-methylimidazole.

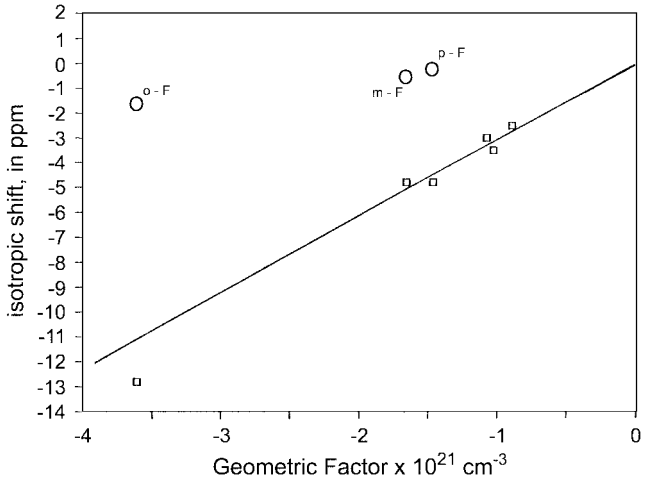

Figure 2. Plot of isotropic shifts for phenyl proton atoms[28] (□) and phenyl fluorine atoms (○) *vs*. the calculated geometric factors for square-planar (TPP)Fe(II)Cl and (F_{20}-TPP)Fe(II) species, toluene-d_8 solvent, 25 °C.

positions. In this instance the meta-signal for the OH^- complex is downfield and that for the Cl^- complex is upfield of the signal for the diamagnetic reference compound. In spite of the correlation between pyrrole proton chemical shift values and the basicity of the axial ligand for five-coordinate anionic complexes, the phenyl fluorine resonances appear to exhibit no systematic trend. Additional variability in ortho-fluoro chemical shift values for high-spin iron(II) complexes is evident for the neutral five-coordinate 2-methylimidazole complex with the signal shifted 10 ppm downfield, and for the six-coordinate bis-THF complex with the ortho-fluoro signal 3 ppm upfield of that for a diamagnetic analogue.

Iron(II) porphyrins also may exist in an unusual "intermediate" spin S = 1 state in the absence of ligands in non-coordinating solvents. Phenyl proton NMR signals for such square-planar species exhibit large shifts (Table 1) due to magnetic anisotropy and associated dipolar shift contributions. Corresponding phenyl F-19 signals show surprisingly small downfield shifts (Table 2), even though the pyrrole proton signal for (F_{20}-TPP)Fe(II) is consistent with the S = 1 formulation.[3]

Low-spin diamagnetic iron(II) complexes of (F_{20}-TPP)-Fe(II) were generated by addition of two piperidine ligands, by CO coordination, and by cyanide coordination. Chemical shift values for these complexes and free-base ligands differ by no more than 1.0 ppm. The F-19 spectrum of (F_{20}-TPP)Fe(II)$(CN)_2^{2-}$ in Figure 1 exhibits only residual multiplet structure due to F-19 spin-spin coupling. A concentration of the reasonably high molecular weight of the complex, the viscous DMSO solvent, and F-19 chemical shift anisotropy at 282 MHz presuambly gives linewidths that are too large for resolution of spin-spin coupling.

Paramagnetic Shift Analysis. Chemical shift values for a paramagnetic substance differ from those of the corresponding diamagnetic complex by a quantity known as the isotropic (or hyperfine) shift value. The carbonyliron(II) tetrakis(pentafluorophenyl) porphyrin, (F_{20}-TPP)Fe(II)CO, was utilized as a diamagnetic reference compound to define the isotropic shift values for the various paramagnetic complexes. The isotropic shift term is composed of the through-bond contact contribution and the through-space dipolar (pseudocontact) terms:[3]

$$\Delta H_{iso}/H = \Delta H_{con}/H + \Delta H_{dip}/H \quad (1)$$

For axial symmetry the dipolar shift can be estimated with the equation:

$$(\Delta H/H)_{dip} = \{(1/3N)(\chi_{//} - \chi_{\perp})(3\cos^2\theta - 1)\}/r^3 \quad (2])$$

where r is the distance of the observed nucleus from the paramagnetic center and is the angle with respect to the z axis for the metal-nuclear vector.[19] The quantity $(3\cos^2\theta - 1)/r^3$ is known as the geometric factor.

In order to gain detailed magnetic and spin delocalization information from NMR spectra, the separation of contact and dipolar terms is a required step. If only the dipolar shift contributes, a plot of isotropic shifts vs. geometric factors (calculated from X-ray molecular structures) for observed nuclei should yield a linear plot with a zero intercept and a slope of $(1/3N)(\chi_{//} - \chi_{\perp})$. This is the case for carbon-13 NMR and proton NMR spectroscopy of certain iron porphyrin complexes.[20-24]

The dipolar shift terms for (F_{20}-TPP)Fe(III)Cl and (F_{20}-TPP)Fe(II) were obtained from proton NMR spectra based on the assumption that there are no significant geometric factor changes between iron tetrakis(pentafluorophenyl)porphyrin complexes and normal iron tetraphenylporphyrin complexes (Tables 3 and 4). The plot of isotropic shifts vs. geometric factors for phenyl fluorines of (F_{20}-TPP)Fe(II) (Figure 2) demonstrates there are large deviations from linearity with the correponding phenyl protons. This suggests that contact shift contributions can not be ignored for the phenyl fluorine signals. In the iron tetrakis(pentafluorophenyl) porphyrin case, large contact shift contributions are observed for the ortho-fluorines.

In conclusion, large chemical shifts for the ortho-fluorine signals of iron tetrakis(pentafluorophenyl)porphyrin complexes were observed. The fluorine-19 NMR chemical shift values depend on the electronic and spin states in the ferric

Table 3. Calculated Dipolar and Contact Shifts for High-Spin Chloroiron(III)Tetraarylporphyrin Complexes

	$(3\cos^2\theta-1)/r^3$ $\times 10^{22}$ cm^{-1}	Calcd[a] $(\Delta H/H)_d$	Obsd $(\Delta H/H)_o$	Net $(\Delta H/H)_c$
(F_{20}-TPP)Fe(III)Cl[b]				
o-F	-4.36	6.3	35.7	29.4
	-2.24	3.2	32.6	29.4
m-F	-1.82	2.6	10.2	7.6
	-1.39	2.0	7.7	5.7
p-F	-1.46	2.1	5.3	3.2

[a]from ref 27. [b]referenced against analogous diamagnetic (F_{20}-TPP)-Fe(II)CO complex at 25 °C. $(H/H)_c$ Contact shift. $(H/H)_d$ Dipolar shift. $(H/H)_o$ Observed isotropic shift.

Table 4. Dipolar and Contact Contributions to Isotropic Shifts for Ferrous Porphyrins

	$(3\cos^2\theta-1)/r^3$ $\times 10^{21}$ cm^{-1}	$(\Delta H/H)_o$	$(\Delta H/H)_d$[a]	$(\Delta H/H)_c$
$(F_{20}$-TPP)Fe(II)[b]				
o-F	-3.6	2.2	11.2	-10.4
m-F	-1.67	0.9	5.0	-4.0
p-F	-1.48	0.3	4.7	-4.5

[a]from ref 27. [b]referenced against the analogous diamagnetic (F_{20}-TPP)Fe(II)CO complex at 25 °C.

and ferrous porphyrins. Analysis of isotropic shifts of the iron(III) porphyrin using fluorine-19 NMR indicates there is a sizable contact contribution at the ortho-fluorine phenyl ring position. Large chemical shift values of the phenyl fluorine, which are sensitive to the oxidation and spin state, can be utilized for identification of the solution electronic structures of iron(III) and iron(II) porphyrins. Large-splittings of ortho- and meta-fluorine signals compared to those of the phenyl proton signals provide useful information about the stoichiometry of ligand binding in that split signals are indicative of asymmetry along the vertical axis of the iron porphyrin complex.

References

1. La Mar, G. N.; Walker, F. A. *The Porphyrins*; Dolphin, D., Ed.; Academic Press: New York, 1979; Vol. IV, p 61.
2. Goff, H. M. *Iron Porphyrins - Part I*; Lever, A. B. P.; Gray, H. B. Eds.; Addison-Wesley: Reading, MA, 1982; p 237.
3. Walker, F. A.; Ursula Simonis, *Biological Magnetic Resonance*; Berliner, L. J.; Reuben, J., Eds.; Plenum Press: 1993; Vol. 12, p 133.
4. Mispelter, J.; Momenteau, M.; Lhoste, J.-M. *Biological Magnetic Resonance*; Berliner, L. J.; Reuben, J. Eds.; Plenum Press: 1993; Vol 12, p 299.
5. Nanthakumar, A.; Goff, H. M. *J. Am. Chem. Soc.* **1990**, *112*, 4047.
6. Chang, C. K.; Ebina, F. *J. Chem. Soc., Chem. Commun.* **1985**, 779.
7. Traylor, P. S.; Dolphin, D.; Traylor, T. G. *J. Chem. Soc., Chem. Commun.* **1984**, 279.
8. Ellis, P. E.; Lyons, J. E. *Coord. Chem. Rev.* **1990**, *105*, 181.
9. Perrin, D. D.; Armarego, W. L. F.; Perrin, D. R. *Purification of Laboratory Chemicals*, 2nd ed.; Pergamon Press: New York, 1980.
10. Furniss, B. S.; Hannaford, A. J.; Rogers, V.; Smith, P. W. G.; Tatchell, A. R. *Vogel's Textbook of Practical Organic Chemistry*, 4th ed.; The Chauer Press, Ltd.: Suffolk, 1978; p 78.
11. Woon, T. C.; Shirazi, A.; Bruice, T. C. *Inorg. Chem.* **1986**, *25*, 845.
12. Guilard, R.; Lecomte, C.; Kadish, K. M. *Structure and Bonding* **1987**, *64*, 205.
13. Nanthakumar, A.; Goff, H. M. *Inorg. Chem.* **1991**, *30*, 4460.
14. Cheng, R. T.; Latos-Grazynski, L.; Balch, A. L. *Inorg. Chem.* **1982**, *21*, 2412.
15. Shin, K.; Kramer, K.; Goff, H. M. *Inorg. Chem.* **1987**, *26*, 4103.
16. Yu, B.-S.; Goff, H. M. *J. Am. Chem. Soc.* **1989**, *111*, 6558.
17. Landrum, J. T.; Hatano, K.; Scheidt, W. R.; Reed, C. A. *J. Am. Chem. Soc.* **1980**, *102*, 6729.
18. Goff, H. M.; Shimomura, E. *J. Am. Chem. Soc.* **1980**, *102*, 31.
19. Horrocks, W. D. *NMR of Paramagnetic Molecules*; La Mar, G. N.; Horrocks, W. D.; Holm, R. H., Eds.; Academic Press: New York, 1973; p 206.
20. Boersma, A. D.; Goff, H. M. *Inorg. Chem.* **1982**, *21*, 581.
21. Goff, H. M. *Biochim. Biophys. Chim.* **1978**, *542*, 348.
22. Walker, F. A.; La Mar, G. N. *Ann. N. Y. Acad. Sci.* **1973**, *206*, 328.
23. Zobrist, M.; La Mar, G. N. *J. Am. Chem. Soc.* **1978**, *100*, 1944.
24. La Mar, G. N.; Eaton, G. R.; Holm, R. H.; Walker, F. A. *J. Am. Chem. Soc.* **1973**, *95*, 63.
25. Cocolios, P.; Lagrange, G.; Guilard, R. *J. Organomet. Chem.* **1983**, *253*, 65.
26. Mispelter, J.; Momenteau, M.; Lhoste, J.-M. *J. Chem. Soc., Dalton Trans.* **1981**, 1729.
27. Minncey, T.; Traylor, T. G. *J. Am. Chem. Soc.* **1979**, *101*, 765.
28. Goff, H, M.; La Mar, G. N.; Reed, C. A. *J. Am. Chem. Soc.* **1977**, *99*, 3641.